37 Spatial modelling of forest community features in the Volzhsko-Kamsky reserve

Rogova, T.V., Chizhikova, N.A., Lyubina, O.E., Saveliev, A.A., Mukharamova, S.S., Zuur, A.F., Ieno, E.N. and Smith, G.M.

37.1 Introduction

This case study illustrates the application of spatial analysis methods on a boreal forest in Tatarstan, Russia. Using remotely sensed data and spatial statistical methods, we explore the influence of relief, soil and climatic factors on the forests of the Raifa section of Volzhsko-Kamsky State Nature Biosphere.

The Raifa area is a challenging area to study relationships between environmental factors and the spatial distribution of vegetation because, even though its climatic variation is minimal, the heterogeneity of its plant cover is high. Its climatic conditions are more similar to a milder taiga subzone further to the south.

Raifa's forests belong to three distinct biocenoses, including southern taiga, broadleaved forests, and mixed forests. Taiga-type forests consist of spruce, fir, pine and larch. At a large spatial scale, the gradient of climatic factors causes zonal replacement of these forest communities; and at a small scale it affects the community structure. Because the compositions of these communities vary so much on the landscape, deciphering which environmental factors are important to these boreal communities requires special spatial analyses that are sensitive to the characteristics of each type of forest.

Separating the large-scale spatial patterns caused by climatic variation from the small-scale patterns caused by stochastic factors or community interactions requires a spatial approach. As pointed out by Legendre and Legendre (1998), field observations often result from a combination of two different processes that account for large-scale and small-scale spatial structuring. The response variable z is spatially structured at a large scale because the explanatory variables are themselves spatially structured by their own generative processes. On the other hand, the deviation of z from the large-scale trend, or the residuals, can result from some stochastic spatial process involving the variable z itself, which causes a lack of independence among the residual components. This is called spatial autocorrelation, and it is generally a function of the geographic distance between sample locations.

To analyse the relationship between environmental factors and the Raifa boreal forest, we created a boreal forest index that should be responsive to the specific environmental factors acting upon this type of forest. The index is defined to be the number of species that belong to a set of boreal species divided by the total number of species at a site. This variable is hereafter referred to as the *boreality*. The model that will be applied assumes that the value of the dependent variable z (boreality) at site j can be presented as the sum of the effect of explanatory variables at site j, a weighted sum of the residuals of the same variable at sites i that surround site j and a random error ε_j. The response variable (boreality) can thus be modelled (in words) as

$$\text{Boreality} = f(\text{Explanatory variables}) + \text{Auto-correlated noise} + \text{noise}$$

The function of the explanatory variables f(Explantory variables) is also called the spatial trend. The last noise component is independently distributed noise. In mathematical terms, the boreality model formula is denoted as

$$z_j = f(\mathbf{X}_j) + \sum_i w_i (z_i - f(\mathbf{X}_i)) + \varepsilon_j \tag{37.1}$$

The first term $f(\boldsymbol{X}_j)$ represents the effects of the explanatory variables $\boldsymbol{X}$ at a site j. It may be the effect of all factors that we assume influence the modelled variable z. These factors may be climatic, such as temperature or wetness, or topographic, such as slope or exposure. In other words, all available data derived from direct measurements or satellite images can be included in $f(\mathrm{X_j})$. The second term in equation (37.1) is the spatial auto-correlation, and it is a weighted sum of the residuals of neighbouring sites. The residuals are obtained by subtracting the effects of the explanatory variables $\boldsymbol{X}$ measured at sites i that surround site j from z. The weight w_i is a function of the geographic distance between location j where we predict variable z and the surrounding locations i. The impact of the surrounding sites is determined by the *range* of the auto-correlation process. Recall from Chapter 19 that the *range* defines the distance between two sites at which there is no more spatial auto-correlation. Hence, a large range means that sites far away from each other are still interacting. The values of the range and weight function w of an auto-correlation are computed through variography analysis, which was described in Chapter 19. The third term in equation (37.1) is the error term and is assumed to be independently normally distributed.

In the context of this study, we assume that the spatial gradients of environmental factors provide large-scale structure of plant cover characteristics, and that the fine-scale spatial heterogeneity of vegetation cover, which is caused by auto-correlated processes, is an intrinsic feature of vegetation itself. Therefore, the main task in this chapter is to apply spatial analysis methods that detect the large-scale spatial gradient of factors reflected in plant cover (the function $f()$), while taking into account the small-scale spatial interaction (the second term in equation (37.1).

37.2 Study area

The study area is in the Volga Valley on a terrace above the flood-lands of the Volga River, ca. 30 km west of Kazan, Tatarstan, Russia (Tajsin 1969, 1972). The western zone of the Raifa section of Volzhsko-Kamsky State Nature Biosphere Reserve is about 7 km in length from north to south (Figure 37.1), and is located within a sub-taiga coniferous-broadleaved forest biogeographical zone. We restricted this study to the western zone of the Raifa because it is the best sampled (see sample locations in Figure 37.1-C); and it exhibits regular replacements of natural territorial complexes from south to north because of changes in latitude, slope, aspect, lithology and moisture (Tajsin 1972). Although the geographic relief of the Raifa area is approximately 60–100 m above sea level and its topography is basically flat, the region contains pronounced erosion features, including ravines and gullies. The mean temperature in the area is 3.4°C, and the mean annual precipitation is 568 mm.

The 3846 hectare Nature Biospere Reserve, which includes the Raifa forests, was created in 1960 to protect unique boreal forests that contain high biodiversity, rare tree species, and a variety of phytocoenosis. The changes in vegetation types over just 2 km within the Raifa section of this preserve are comparable with what can be observed over a 100-km section of European Russia.

Figure 37.1. A: The location of Tatarstan. B: The location of the Raifa reserve in Tatarstan. C: Study area of forest types, on the basis of species domination (Porfiriev 1968). The extent of the study area is 7.2 km from north to south, and 2.7 km from east to west. Lake Raifskoe is in the centre of the region, with the Sumka River flowing into the lake from the northeast (not plotted on the study area map). Each dot in panel C represents a sample site. The shading corresponds to different forest types. Grey colouring in the study area indicates the degree of boreal species (dark corresponds to higher values).

The predominant species in Raifas' forest community is *Pinus sylvestris.* The communities also includes representatives of taiga and broadleaved zones, such as *Quercus robour, Tilia cordata, Betula pendula, Alnus glutinosa, Pinus silvestris, Piceax fenica* and more rarely, *Abies sibirica.*

37.3 Data exploration

A total of 534 geobotanical sites were sampled for this study (Figure 37.1C). Vascular plant community compositions were sampled using 100-m^2 plots in June of 2000–2004. In all, 485 vascular plant species were recorded, and 327 of them were present in more than three sites. The total number of boreal species found on the plots amounts to 22 species (Bakin et al. 2000). The proportion of these boreal species to species of all coenosis groups at each site, i.e., the site's *boreality*, ranged from 0% to 60%. The Cleveland dotplot (see Chapter 4) shows that no sites have extremely high values of boreality (Figure 37.2), but there are many observations with boreality equal to zero.

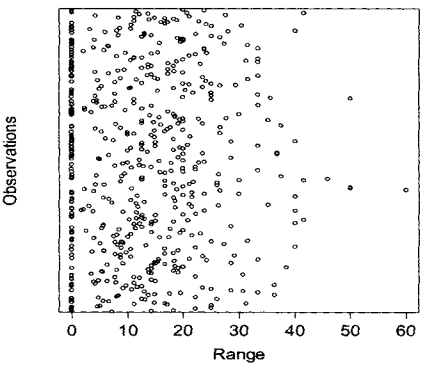

Figure 37.2. Cleveland dotplot for boreality. The vertical axis shows the observations in the order as they were in the spreadsheet, and the horizontal axis gives the value.

Four remotely sensed variables, derived from the LANDSAT 5 satellite images that were taken on June 22, 1987, were used as explanatory variables, namely:

1. The normalised difference vegetation index (NDVI). Positive values of NDVI indicate green vegetation; negative values indicate non-vegetated surface features, such as water, barren rock, ice, or snow.
2. Temperature in degrees Kelvin (Temp).
3. Index of Wetness (Wet). The index of wetness ranges from −1 to 1. Positive values indicate water surfaces; negative values correspond to wet habitats.

4. Index of Greenness (Grn). The index of greenness ranges from −1 to 1. Larger values correspond to more dense vegetation cover.

In addition to the data derived from satellite images, we also used latitude (X) and longitude (Y) of the sites as explanatory variables, assuming that they represented an indirect relationship with climatic gradients.

A pairplot for the four satellite variables and the two spatial coordinates is presented in Figure 37.3. All variables have some outliers and show collinearity. One site has outliers in nearly all variables. Temp has two additional sites with outlier values. Correlations between the latitude X, and longitude Y variables and the satellite variables are relatively low (<0.4). The correlations between the remotely sensed variables (see lower diagonal panels in Figure 37.3) all have serious collinearity issues, even after removing the outlier.

To detect collinearity (Chapter 5) between *all* explanatory variables, we calculated pair-wise correlations between the six variables and variance inflation factors (VIFs). Recall that VIF values were used in Chapter 26 to assess collinearity, and the reader is referred to that chapter for a detailed explanation of their calculation and interpretation. Basically, high VIF values, say >5 or >10, are an indication of collinearity. The VIF values for all six variables were X (1.365), Y (1.450), Temp (1.882), Wet (4.929), NDVI (13.564) and Grn (19.461). The VIF values for index of greenness and NDVI in this study indicate serious collinearity. Both of these variables reflect vegetation cover density. Based on these VIF values (and those obtained by dropping Grn), we decided to omit NDVI and Grn from further analysis. As a result, the remaining variables all have correlations smaller than 0.8.

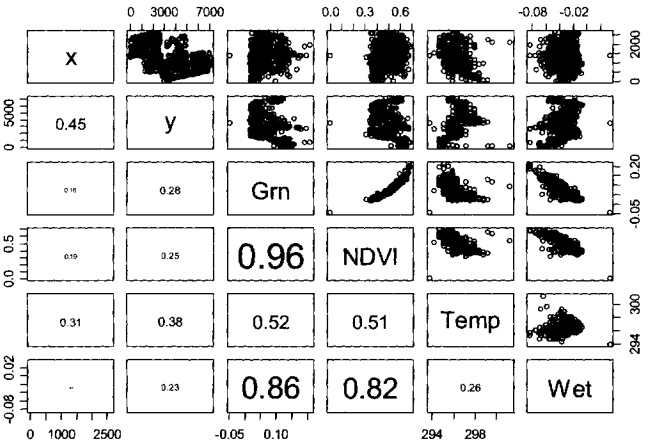

Figure 37.3. Pairplot of the two spatial variables and the four satellite variables. The lower diagonal elements contain the (absolute) correlations, and the font size is proportional to the value. All variables have outliers and show collinearity.

37.4 Models of boreality without spatial auto-correlation

To capture how much the boreality index varies with environmental factors, two different models were applied and their results compared. One was a linear regression model (LM). The other was an additive model (AM) with Gaussian error distribution. We examined the LM and AM models with different sets of predictors (i.e., the set of spatial coordinates and the set of remotely sensed data) to obtain insight into the importance of each explanatory variable. Remotely sensed variables and spatial coordinates were added to each model one at a time, and the relevance of each predictor in the individual models was investigated using an F-test for nested models (Chapters 5 and 7). Figure 37.4 shows one example of an AM model in which X, Y, Temp and Wet were used as explanatory variables. It has a pattern of increasing residual spread for larger fitted values, which indicates a violation of the homogeneity assumption. The same pattern was encountered in all LM and AM models; therefore, all violated assumptions of homogeneity. To proceed further, we have several options, namely:

- Apply a data transformation on boreality. As long as a monotonic transformation is applied, it makes biological sense to do this (or formulated differently, it is not biological nonsense to apply a transformation on boreality percentages).
- Boreality is defined by the numbers of species that belong to a set of boreal species divided by the total number of species at a site. Hence, we have S_i successes out of n_i trials, which can be modelled as a Binomial GLM or GAM (Chapter 6).
- The number of species belonging to the boreal coenosis species can be modelled as a Poisson GLM or GAM with the number of species per site as an offset variable (Chapter 6).
- Model the heterogeneity in terms of spatial covariance of the error component.

There is no perfect solution, so any of these approaches can be applied to a given dataset. Some may work; some may not work. We decided to transform boreality (because it worked) according to the following transformation:

$$z_i = (1000(S_i + 1)/n_i)^{1/2}$$

where z_i is transformed boreality, S_i is the number of species that belong to boreal coenosis species, and n_i is the number of all species at the site i. See Cressie (p. 395, 1993) for a discussion of this transformation, and other types of transformations (i.e., the Freeman–Tukey transformation). The effect of the transformation for the LM and AM can be seen in Figure 37.5. All explanatory variables selected in the data exploration step were used in these models, and except for the coordinate X, all variables were significant at the 99% confidence level (Table 37.1).

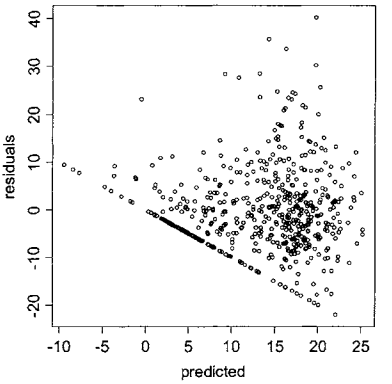

Figure 37.4. Residuals versus fitted values. The residuals were obtained from an AM model containing *X*, *Y*, Temp and Wet as explanatory variables. Cross-validation was used to estimate the optimal amount of smoothing for each term.

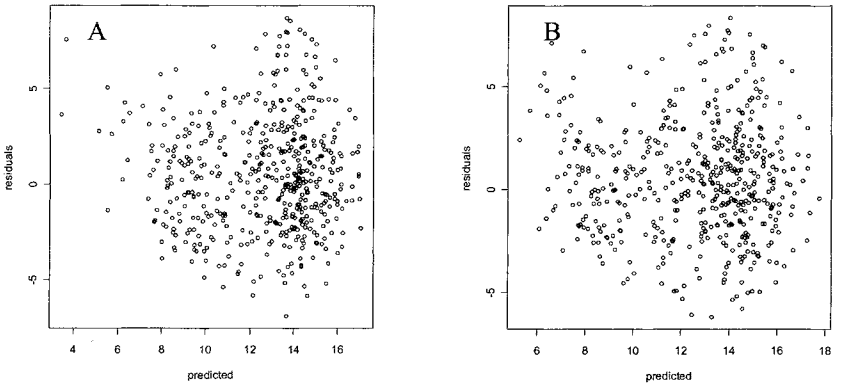

Figure 37.5 Residuals versus fitted values from a model containing Y, Temp and Wet as explanatory variables. A: The residuals were obtained from the LM model. B: The residuals were obtained from the AM model. AM residuals show better accordance with the homogeneity assumption. In both panels boreality was transformed.

Table 37.1. *p*-values for the explanatory variables. RS stands for remote sensing.

	X	*Y*	Temp	Wet
LM(*X*,*Y*)	0.083	<0.001		
LM(RS data)			<0.001	<0.001
LM(*X*,*Y*, RS data)	0.045	<0.001	<0.001	<0.001
AM(*X*,*Y*)	0.842	<0.001		
AM(RS data)			<0.001	<0.001
AM(*X*,*Y*, RS data)	0.157	<0.001	<0.001	<0.001

We regarded site position on the north-south axis (coordinate *Y*) as a factor that reflects the spatial (zonal) gradient of environmental factors. Table 37.1 shows that the *Y* coordinate is highly significant in both the LM and the AM. This result can be considered as a confirmation of our assumption regarding the large-scale spatial trend of boreality. The variable *X* is not important in any of the models, probably because the extent of explored territory in this direction is too small to reveal any serious environmental trends. We decided to remove the *X* coordinate from further analyses.

Because all remaining explanatory variables are significant in the models, there is no point in doing any further model selection. In the next section, we will improve upon these models by taking into account spatial auto-correlation. We will use two models, namely (i) the LM based on *Y* coordinates of site locations, temperature and index of wetness; and (ii) the AM based on *Y* coordinates of site locations, temperature and index of wetness, and we will add spatial auto-correlation (i.e., values for the second term in our boreality equation 37.1)

37.5 Models of boreality with spatial auto-correlation

The models discussed in the previous section can reveal spatial trends of environmental factors in boreality. Recall from equation 37.1 that the term 'spatial trend' refers to the effect of the explanatory variables. However, not all variability in boreality is explained by the spatial trend. One way to show how much is not explained is to calculate the correlation between observed and fitted values for each model. For the AM, this correlation was 0.697. We can try to improve these models by taking into account spatial auto-correlation. We can add spatial correlation structure in several ways, and we discuss two options here. The first option is to use an iterative scheme, as described in Bailey and Gatrell (1995). It works in the following way:

1. Start with an LM or AM without correlation structure and obtain residuals.
2. Estimate the residual covariance structure from the variography analysis (Chapter 19) and incorporate this in the model using a generalised least squares (GLS) approach (Chapters 5, 16, 26). Recall that GLS is an estimation procedure that allows for a non-diagonal error covariance matrix in linear regression or additive modelling.
3. Get new residuals and re-estimate the covariance structure.

4. Repeat steps 2 and 3 until convergence.

The second option is to estimate the spatial trend and correlation structure simultaneously using numerical optimisation of the likelihood function (Pinheiro and Bates 2000). In this chapter, we will discuss both approaches.

The Bailey and Gatrell scheme

We subtract the LM spatial trends from the observed boreality to obtain the residuals and use these in *variography* or *variogram analysis*. Because the variography analysis is based on the assumption of multivariate normality and stationarity of the residuals (in this case), we need to verify that the residuals meet these assumptions before continuing.

With stationarity, we mean the so-called second-order stationarity (Chapter 19), which can be checked by testing for spatially varying mean and variance, and heterogeneity of spatial covariance. Because we have already subtracted the LM and spatial trend from the observed boreality, the residuals have zero mean.

To test the LM residuals for departure from stationarity and multivariate normality, we use the *h*-scatterplot. This tool is used to plot the residuals in points $\boldsymbol{s}_1$ against residuals in points $\boldsymbol{s}_2$ separated by distance lag $\boldsymbol{h}$. To be more precisely, for each observed site in the study area, we can obtain a list of sites that are *exactly* $\boldsymbol{h}$ units away from it. Call this collection of points E. It may be an option to use $\boldsymbol{h}$ plus/minus a small number or else E only contains a few or no points at all. In an *h*-scatterplot, we plot the value of the residual at $\mathbf{s}_1$ along the x-axis and the values of the residuals in E along the y-axis. This whole process is then repeated for each site. The point $\mathbf{s}_1$ is also called the head and $(\boldsymbol{s}_1+\boldsymbol{h})$ the tail. If the distribution of the residuals is highly skewed, then small values of residuals in heads correspond to big values of residuals in tails and vice versa. If this is the case, then the *h*-scatterplot will display a so-called 'butterfly wing', i.e., groups of points that are far away from the diagonal line. *h*-scatterplots for LM residuals are presented in Figure 37.6. We used two different lags: 200 and 800 m. Both graphs indicate that there is no clear butterfly wing effect. If the points follow the diagonal line, then there is positive correlation (high values of the residuals at both $\mathbf{s}_1$ and $(\boldsymbol{s}_1+\boldsymbol{h})$). In this case, there is no clear trend.

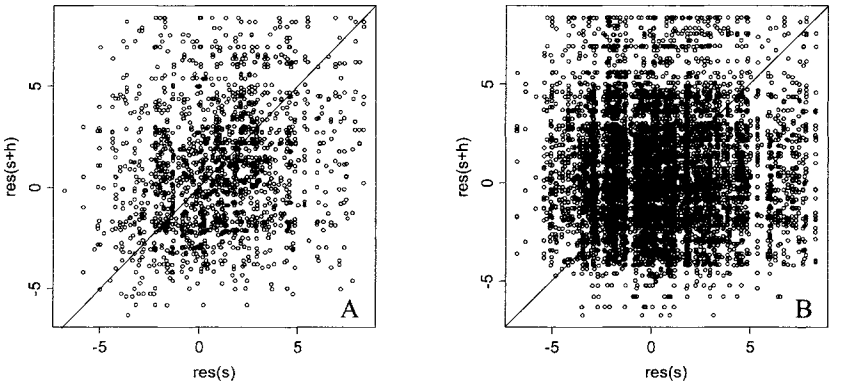

Figure 37.6. *h*-scatterplots. A: Plot for LM(ce) residuals for lag $h = 200$ m. B: Plot for LM(ce) residuals for lag $h = 800$ m. The value of the residual at $\mathbf{s}_1$ is along the horizontal axis, and residuals of all points that are **h** units away from $\mathbf{s}_1$ are plotted along the vertical axis.

Another way to assess the multivariate normality assumption of the residuals is to verify one-dimensional normality by using QQ-plots (Chapter 4). For these data, the *h*-scatterplots and QQ-plot indicate that the stationarity and normality assumptions are valid. Therefore, we can proceed with variography analysis and use geostatistical means to model the boreality residuals.

Recall from Chapter 16, that when we applied GLS on time series data, we had to specify the type of auto-correlation structure. Options were the AR(1), ARMA(*p*,*q*), and compound symmetry structure, among others. A useful tool to decide between the various temporal auto-correlation structures was the auto-correlation function. In spatial statistics, we have the same problem. The spatial equivalent of the auto-correlation function is the variogram, or, more precisely, the *semi-variogram*. It is a measure of spatial dependence between boreality in point $\boldsymbol{s}_1$ and $\boldsymbol{s}_2$. These points are *separated* by the distance $\boldsymbol{h}$, with the direction from $\boldsymbol{s}_1$ to $\boldsymbol{s}_2$. The estimated variogram (using sample data) is referred to as the *empirical variogram* or sometimes as the *sample variogram*. The mathematical formulation of the variogram and its estimator are given in Chapter 19.

Based on the shape of the variogram we can choose an appropriate error structure for the GLS. Common options are the exponential, Gaussian, linear and spherical models. Figure 19.11 in Chapter 19, Figure 5.9 in Pinheiro and Bates (2000) or Figure 13.8 in Legendre and Legendre (1998) show the corresponding shapes of the variogram for these models. So, we need to make a variogram for the residuals (sample variogram), and decide which model for the error structure is the most appropriate (i.e., which model fits the sample variogram best). In Figure 37.7, the sample variogram graph (dots) for LM residuals shows that two variogram models may be appropriate: spherical and exponential. To decide which of these models fits the sample variogram best, we can fit both models and compare their weighted sum of squares, i.e., the sum of distances between fitted

variogram values and sample variogram values. The smaller sum of squares indicates the better fit.

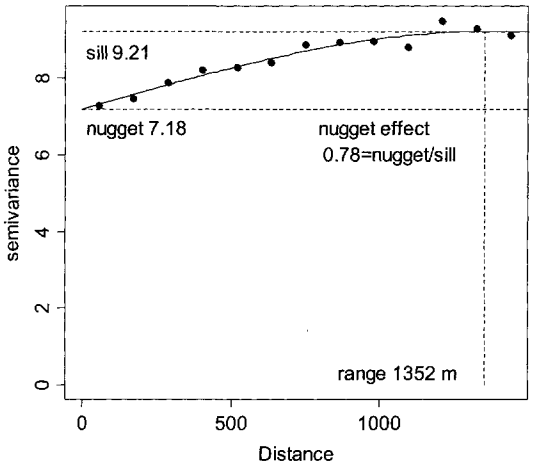

Figure 37.7. Graph of sample variogram and initial spherical correlation structure for LM residuals.

All variograms have a couple of unknown parameters that we need to estimate. The line can be characterised by the following parameters (Figure 37.7): the *range* of the spatial auto-correlation and the *nugget effect*. The *range* of the variogram model gives the maximum distance of site-to-site influence. The *nugget effect* is the variance of the difference between values at the sites that are co-located, or so close in space that we can consider them as one location. It is expressed as a proportion of the sill (but this may depend on software). *Sill* is half of the maximum variance of the difference between values at different locations.

For the residuals obtained from the LM and AM, we fitted both spherical and exponential variogram models. The spherical variogram model had the better fit (its sum of squares was smaller). Therefore, we will only present results obtained with the spherical variogram model.

Based on Figure 37.7, we assume (initially) that the range is 1352 m and the nugget is 0.78 (expressed as a fraction of the sill). The nugget effect plays a role similar to the R^2 in linear models; not more than 28% (= 1 − 0.78) of the variance in the data at any given location can be explained using data in other locations. In other words, only 28% of the variance of boreality residuals can be explained by auto-correlation process. These parameters of the correlation structure are just initial estimates, because we used the residuals of the LM trend model to estimate them. So, following the iterative scheme described by Bailey and Gatrell, we need to (i) incorporate these parameters into the model by specifying the range and nugget effect, and (ii) get new residuals and re-estimate the covariance structure by fitting the variogram model to the newly calculated sample variogram of these

residuals. Steps (i) and (ii) are repeated until the spatial correlation parameters converge. The spherical data correlation structure in the final LM(ce) trend model obtained by this iterative scheme has a range of 1549 m, and the nugget effect is 0.66 (nugget is 6.66 and sill is 10.13). Note that these values differ from the initial values.

In time series analysis, time's only direction is forward. In spatial statistics, the lag can be in any direction. So far we have assumed that the relationship between two sites that are separated by a distance $\boldsymbol{h}$ is the same whatever the direction of $\boldsymbol{h}$ is. The term *anisotropy* is used when the strength of the spatial auto-correlation process is not the same in all directions; in some directions the strength is stronger and in some it is weaker. As the GLS model that was used to incorporate the data correlation structure *assumes* isotropic auto-correlation (where the strength *is* the same in each direction), we need to verify this assumption.

To detect anisotropy, we can look at the behaviour of empirical variograms for the separation vector $\boldsymbol{h}$ taken only along selected directions. These are so-called directional variograms. In Figure 37.8 empirical directional variograms of LM(ce) residuals are presented. Four directions were used: 0°, 45°, 90° and 135°. The direction angle is evaluated as the angle between the y-axis and the selected direction.

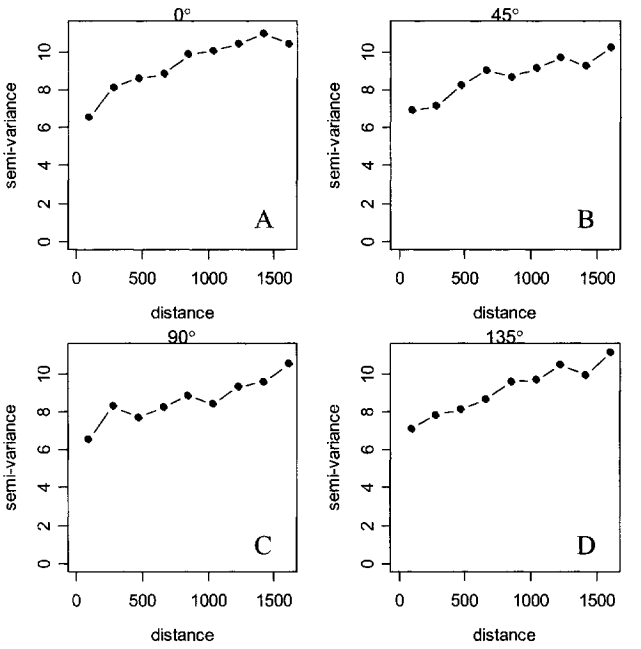

Figure 37.8. Empirical directional variogram for LM(ce) residuals for $\boldsymbol{h}$ distances. A: for the 0° direction, B: for the 45° direction, C: for the 90° direction, D: for the 135° direction.

We can identify anisotropy if there is a difference between slopes of the curves that join values of sample variograms. A visual inspection may reveal anisotropy if the variogram values increase fast in some directions and more slowly in others. In this case, there is some evidence of anisotropy at the 45° and 90° directions, but it is not strong so it is difficult to see a clear difference between these empirical variograms. We can detect anisotropy numerically by fitting variogram models to two directional empirical variograms that have perpendicular directions. The first variogram must have the flattest curve (as judged by eye), and the second variogram must have a perpendicular direction.

Here, we use two directional empirical variograms for the 0° and 90° directions, and Figure 37.9 shows the corresponding empirical variograms (dots) with fitted spherical variogram models. Anisotropy is characterized by two parameters: the anisotropy angle and the anisotropy ratio. The anisotropy angle is the direction of the variogram with the flattest curve and greater range (here it is the 90° one). The anisotropy ratio is the ratio of greater range to the smaller range.

The fitted spherical variogram models for LM(ce) residuals in Figure 37.9 have a nugget effect 0.60 (sill 10.60 and nugget 6.38). It is slightly smaller than the nugget effect determined without taking into account anisotropy (0.66). The direction with the greater range was 90°, and the range was 2185 m (Figure 37.9-A). The smaller range equals 1411 m (direction 0°, Figure 37.9-B). The anisotropy ratio is 2185/1419 ≈ 1.55, so the auto-correlation of sites along the 90° direction diminishes with distance in 1.55 times slower than along the 0° direction.

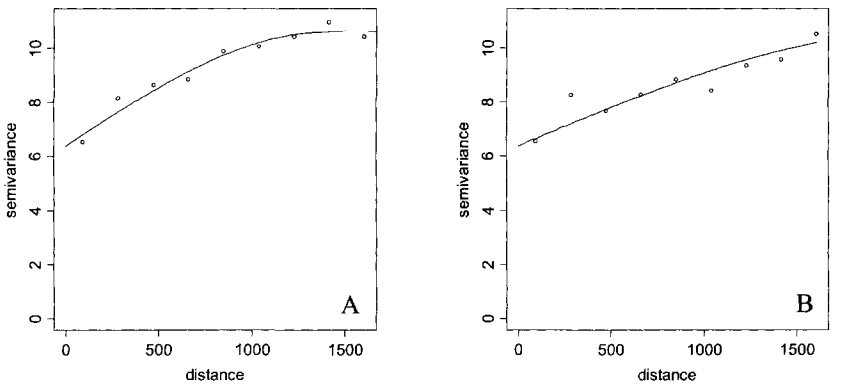

Figure 37.9. Empirical variograms (dots) with fitted variogram models (line). A: Empirical directional variogram for LM(ce) residuals along the 0° direction and fitted exponential variogram model with range 1411 m, sill 10.60 and nugget 6.38. B: Empirical directional variogram for AM(ce) residuals along the 90° direction and fitted exponential variogram model with range 2185 m, sill 10.60 and nugget 6.38. This means that the variogram value of co-located sites is 6.38 and the variogram values of sites separated by more than approximately 1411 m along the 0° direction and more than 2185 m along the 90° direction is assumed equal to 10.60.

Approach 2: Numerical optimisation of the likelihood function

In the approach described above, the Bailey and Gatrell iterative scheme was used to estimate the trend component and the correlation structure. We now briefly describe how to estimate the spatial trend and correlation structure simultaneously using numerical optimisation of the likelihood function (Pinheiro and Bates 2000). We will apply it to the AM trend model, obtain the AM(ce) model and inspect its residuals by variography analysis to detect anisotropy of the auto-correlation process.

Before applying the numerical optimisation routines, we inspected (using the same tools as above, e.g., QQ-plots and *h*-scatterplots) the boreality residuals obtained by the AM trend model to check multivariate normality and stationarity. Both assumptions were valid. We then applied the numerical optimisation routines to estimate the spatial trend component and correlation structure simultaneously. This model uses the same variogram models. We can specify different spatial auto-correlation structures and then compare them using the AIC. The smallest AIC shows the most adequate data correlation model. Just as before, we compared spherical and exponential models. The AIC were nearly equal, but we decided to use the spherical model.

A spherical data correlation structure was specified for the AM(ce) with the following starting values: *range of auto-correlation* 821 m and *nugget effect* 0.70.

The software that we used (nlme library in R) scales the maximum variance (sill) to one, and as a result we can only obtain relative values of the nugget effect. If the aim of the analysis is to model the spatial trend and take into account the spatial auto-correlation, then we need the exact values of nugget and sill.

The models used above, the AM(ce), LM(ce), and the GLS in the Bailey and Gatrell scheme, can only cope with isotropic spatial auto-correlation (due to software implementation). So, after convergence of the estimation methods, we need to check the residuals for anisotropy, and this can be done in the same way as above. For the AM(ce) residuals, anisotropy was detected along the 90° direction (the greater range along the 90° direction is 1227 m, and the smaller range along the 0° direction is 752 m. The anisotropy ratio is $1227/752 \approx 1.63$. The nugget is 6.3 and sill 9.1. So the nugget effect determined by variography analysis ($0.69 = 6.3/9.1$) is close to the nugget effect obtained by the numerical optimisation.

37.6 Conclusion

After applying several different spatial models, we conclude that it is possible to detect the spatial trend of environmental factors in plant cover, even if the vegetation is spatially heterogeneous. Remote sensing data are important to estimate the spatial distribution of specific species and plant community features.

The process of spatial analysis involves many steps to find the best spatial model that describes the relationship between environmental factors and site vegetation (Figure 37.10). The process consists of data exploration, model creation based only on environmental factors, and model refinement to take fine-scale sto-

chastic and local interactions due to auto-correlation into account. The AIC for the optimal linear regression model without an auto-correlation structure was 2507, and using the Bailey and Gatrell scheme, LM(ce), gave AIC = 2478. For the AM and the AM(ce) using the numerical optimisation gave AIC = 2622 and AIC = 2461 respectively. Hence, incorporating a spatially correlated, stochastic component of vegetation variability (presented as residuals) into each model improve its measures of fit.

Information about anisotropy (obtained by variogram analysis of residuals) can help us to make some inferences on the local spatial behaviour of the investigated variable. The anisotropy angle was 90°, which means that along this direction the spatial auto-correlation diminishes more slowly than in the 0 ° direction. Disregarding the anisotropy may overestimate or underestimate the variable in some directions, and as a result it may give an improper spatial picture of the phenomenon.

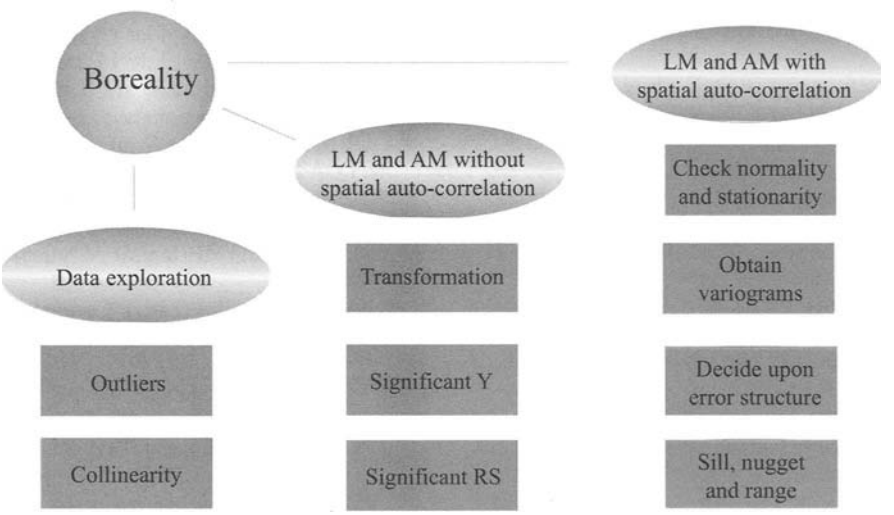

Figure 37.10. Outline of the data analyses. The data exploration indicated the presence of outliers and collinearity. We then applied linear regression and additive modelling and assumed that the error component was independently distributed. All explanatory variables in this model were significantly different from 0 at the 5% level, except for the X coordinate. We continued the analysis by allowing for a residual spatial correlation dependency. Using a sample variogram it was decided to use a spherical correlation structure. The resulting model can be written as: Boreality = F(Explanatory variables) + spatial correlated noise. The advantage of this model is that we are less likely to commit a type I error because we allow for spatial dependency.

Acknowledgement

We would like to thank Neil Campbell and Pam Sikkink for useful comments on an earlier draft.